

Swift observations of the 2015 outburst of AG Peg – from slow nova to classical symbiotic outburst

Gavin Ramsay¹, J. L. Sokoloski², G. J. M. Luna³, N. E. Nuñez⁴

¹Armagh Observatory, College Hill, Armagh, BT61 9DG, UK

²Columbia Astrophysics Lab, 550 W120th St., 1027 Pupin Hall, MC 5247 Columbia University, 10027, New York, USA

³Instituto de Astronomía y Física del Espacio (IAFE, CONICET-UBA), Av. Inte. Güiraldes 2620, C1428ZAA, Buenos Aires, Argentina

⁴Instituto de Ciencias Astronómicas de la Tierra y el Espacio (ICATE-UNSJ), Av. Espanã (sur) 1512, 5400, San Juan, Argentina

Accepted 2016 June 23. Received 2016 June 23; in original form 2016 April 5

ABSTRACT

Symbiotic stars often contain white dwarfs with quasi-steady shell burning on their surfaces. However, in most symbiotics, the origin of this burning is unclear. In symbiotic slow novae, however, it is linked to a past thermonuclear runaway. In June 2015, the symbiotic slow nova AG Peg was seen in only its second optical outburst since 1850. This recent outburst was of much shorter duration and lower amplitude than the earlier eruption, and it contained multiple peaks – like outbursts in classical symbiotic stars such as Z And. We report Swift X-ray and UV observations of AG Peg made between June 2015 and January 2016. The X-ray flux was markedly variable on a time scale of days, particularly during four days near optical maximum, when the X-rays became bright and soft. This strong X-ray variability continued for another month, after which the X-rays hardened as the optical flux declined. The UV flux was high throughout the outburst, consistent with quasi-steady shell burning on the white dwarf. Given that accretion disks around white dwarfs with shell burning do not generally produce detectable X-rays (due to Compton-cooling of the boundary layer), the X-rays probably originated via shocks in the ejecta. As the X-ray photoelectric absorption did not vary significantly, the X-ray variability may directly link to the properties of the shocked material. AG Peg’s transition from a slow symbiotic nova (which drove the 1850 outburst) to a classical symbiotic star suggests that shell burning in at least some symbiotic stars is residual burning from prior novae.

Key words: Stars: individual: AG Peg; Stars: binaries – symbiotic – winds and outflows; Physical data and processes: accretion and accretion discs – instabilities

1 INTRODUCTION

Symbiotic Binaries have orbital periods with timescales of years and contain a cool giant star which is losing mass, typically via a wind, to a hot compact star (see Allen 1984, Kenyon & Webbink 1984 and Mikolajewska 2007). The evolution of these systems has long been debated (e.g. Iben & Tutukov 1996), but there is now a growing appreciation that symbiotic binaries could produce some fraction of supernovae Ia outbursts (e.g. Di Stefano 2010, Dilday et al. 2012).

In their catalogue of symbiotic stars, Belczyński et al. (2000) list more than 200 known or suspected symbiotic stars, with more being discovered through surveys such as IPHAS (Corradi et al. 2008, 2010, Rodríguez-Flores et al. 2014). The optical photometric characteristics of symbiotic stars are diverse. Symbiotic stars can show ‘classical’ outbursts lasting weeks to years where they brighten by $\sim 1\text{--}2$

mag. It is unclear if most of these outbursts are due to nuclear burning on the surface of the white dwarf or an accretion disk instability of the sort seen in some cataclysmic variables (CVs) such as dwarf novae or a combination of both nuclear burning and a disk instability (as in Z And, Sokoloski et al. 2006). There are other symbiotic stars which show outbursts which are powered by thermonuclear runaways (TNRs), including slow novae where the outburst event can extend for many decades (e.g. Allen 1980, Kenyon & Truran 1983).

Observations made using the *Einstein* and *ROSAT* satellites showed that symbiotic stars are X-ray emitters at relatively low flux levels when in a quiescent state (Allen 1981, Mürset, Wolff & Jordan 1997). Luna et al. (2013) made a survey of symbiotic stars using the X-ray telescope (XRT) on-board the *Swift* satellite and found (as did Mürset et al. 1997) that they could group the sources into those which

arXiv:1606.07397v1 [astro-ph.HE] 23 Jun 2016

had very soft X-ray spectra (originating from shell burning on the surface of the white dwarf); those which had emission extending to ~ 2.4 keV (probably due to the collision of winds from the red giant and white dwarf); and those which showed emission above ~ 2.4 keV. Whereas Mürset et al. (1997) ascribed the hard X-rays to accretion onto a neutron star, Luna et al. (2013) attributed the thermal hard X-ray emission, as detected using the *Swift* XRT, to boundary layer emission around a white dwarf. Inevitably some sources showed X-ray spectra combining characteristics of more than one of these classes. These observations were generally made when the symbiotic binary had been in quiescence and not in outburst.

Most X-ray observations of symbiotic stars have typically been made at only one epoch. In contrast, observations of the symbiotic nova AG Dra made using *ROSAT* in 1994 show that the X-ray flux decreased over the course of the optical outburst (which was also noted in an earlier minor outburst using *EXOSAT* observations) which was attributed to the decrease in the temperature of the hot component, possibly due to an increase in the apparent size of its outer envelope (Greiner et al. 1997). An anti-correlation between the optical and X-ray flux over an outburst has also been seen in dwarf novae (e.g. Wheatley et al. 1996) and in the double degenerate interacting helium binary KL Dra (Ramsay et al. 2012).

The symbiotic binary AG Peg is one example of a slow symbiotic nova, which has a photometric record extending more than 200 years. At the beginning of the 19th century AG Peg was recorded as a ~ 9.5 mag star which experienced a gradual brightening around 1850, reaching ~ 6 mag 20 years later (Rigollet 1947, Belyakina 1968). (Mürset & Nussbaumer 1994 show the light curve of AG Peg extending over 150 years.) Observations made by amateur astronomers whose records are accessible on-line (e.g. AAVSO¹ and BAAVSS²) date back to 1941. These show that AG Peg made a slow decline in brightness and only reached its pre 1850 outburst by the end of the 20th century. Indeed, there is evidence that the 1850 outburst was the slowest nova outburst ever recorded (e.g. Kenyon, Proga & Keyes 2001).

As AG Peg is a relatively bright object, it was studied spectroscopically by the end of the 19th century, showing a range of emission and absorption lines whose characteristics changed over months and decades. Later observations show the binary orbital period is 818.2 ± 1.6 d with an eccentricity of 0.11 (Merrill 1951, Fekel et al. 2000). The spectral type of the giant star is M3 III (Kenyon & Fernandez-Castro 1987), while the mass function of the system is consistent with the hot component being a white dwarf (Fekel et al. 2000).

There was some indication in May 2013 that AG Peg was beginning a new active phase when it was reported that AG Peg had brightened by ~ 0.3 mag (Munari et al. 2013). However, during June 2015 it was found that AG Peg had brightened from $V \sim 8.5$ to $V \sim 7.0$ over the course of a few weeks (Waagen 2015). Based on the long term light curve shown in Mürset & Nussbaumer (1994) and the records of the amateur astronomer groups mentioned earlier, we con-

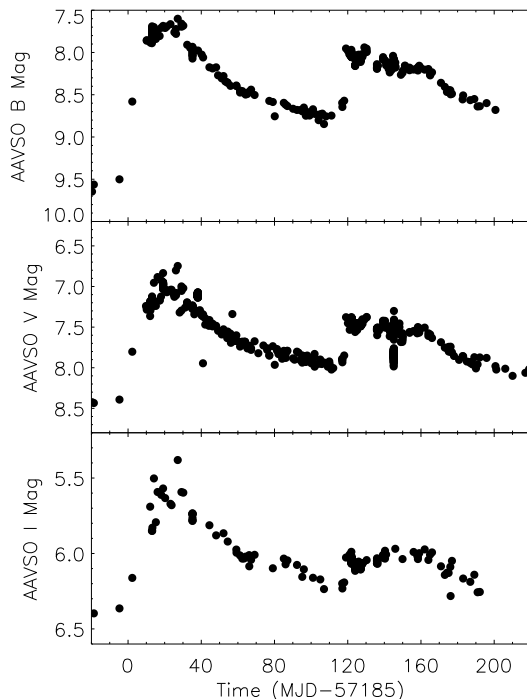


Figure 1. Photometry of AG Peg over the outburst in the *BVI* bands and taken from AAVSO data (Kafka 2015). We have not attempted to remove potentially discrepant data points. The outburst started on MJD=57185 which corresponds to 2015 June 12.

sider it highly unlikely that an outburst of the duration and amplitude of the 2015 outburst has taken place on AG Peg since the early 1940's, and the 2015 outburst is therefore likely to be the first *bona fide* outburst since the 19th century. However, we cannot exclude the possibility that a short duration event took place, for instance during the intervals when AG Peg was close to the Sun and therefore not observable.

We requested Target of Opportunity observations using *Swift* shortly after the announcement of the 2015 eruption and these observations showed that AG Peg was detected in X-rays during the optical outburst (Luna et al. 2015, Ramsay et al. 2015). Since these early observations, *Swift* has been used to observe AG Peg at regular intervals. The main goal has been to determine how the X-ray flux (and spectrum) changes over the outburst and compare it with the observations of other accreting white dwarfs.

2 OVERVIEW OF OBSERVATIONS MADE BY AMATEUR OBSERVERS

2.1 Photometry

Observations made by amateur astronomers (e.g. AAVSO and BAAVSS) show that AG Peg was at $V \sim 8.5$ mag on 2015 June 6, reaching $V \sim 7.5$ by June 21 and reached a peak of $V \sim 6.8$ mag by the end of June (Figure 1). Over the next 40 days it declined by half a magnitude after which it declined more slowly, reaching a plateau phase at $V \sim 7.8$ mag. Around Oct 10 AG Peg showed a 're-brightening' event reaching $V \sim 7.5$ mag after ~ 20 days, after which it started to decline. The peak magnitude of the June outburst was ~ 1

¹ <http://aavso.org>

² <http://britastro.org/vssdb>

mag fainter than it was in 1870 and the rate of decline in this current outburst appears much quicker (e.g. Belyakina 1968). The amplitude of the outburst is higher in the *B* band (~ 1.8 mag) compared to the *I* band (~ 0.9 mag). These data also show the re-brightening event ($V \sim 0.5$ mag) occurred on a timescale of less than 1 d and was relatively brighter at bluer wavelengths compared to the June 2015 outburst.

2.2 Spectroscopy

AG Peg was observed using the LOTUS NUV-optical spectrograph on the Liverpool Telescope on 2015 July 1 (approximately 20 days after of the start of the outburst). Compared to pre-outburst spectra, the relative strength of O and N emission lines relative to the Balmer lines was stronger during the outburst (Steele et al. 2015).

Many groups, including amateur astronomers³, have made spectroscopic observations of AG Peg over its outburst. These observations show strong emission lines, including the Balmer series plus He I (6678) and He II (4686), [O III] (4363) and the O VI emission band at 6825 Å, which is due to Raman scattering. A full analysis of the optical spectra made over the course of the outburst is beyond the scope of this work, but we were able to estimate the effective temperature of the ionizing source using the He II (4686) and H β lines and the formula of Iijima (1981) (quoted in Sokoloski et al. 2006) which derives the effective temperature using the equivalent width (EW) of these lines (we ignore the He I (4471) line since it is much weaker than He II and H β).

We used spectra taken by amateur astronomers⁴ which covered the He II (4686) and H β lines to derive their EW (we estimated that the error on the EW measurements was ~ 10 percent by making a number of measurements of the same line). This shows that the EW of He II (4686) was somewhat variable over the outburst but showed a distinct decrease at the time of the optical re-brightening event (Figure 2). This decrease is also seen in the EW of the H β line, although there is a trend for the EW to increase over the course of the outburst. We show the relative temperature over the course of the outburst in Figure 2 which shows that the effective temperature of the ionizing source decreases over the duration of the outburst.

3 SWIFT OBSERVATIONS

3.1 Overview

The *Swift* satellite was launched in 2004 with a primary goal of detecting gamma-ray bursts, and locating and characterising their X-ray and optical/UV properties (Gehrels et al. 2004). NASA runs a Target of Opportunity programme which provides the means for observing targets which have unexpectedly become interesting (novae for instance) at the earliest opportunity. Observations of AG Peg were made using *Swift* on 2015 June 28th. Given the brightness of the source, it was saturated in the UVOT instrument (we discuss the implications of this in §4.3).

³ e.g. <http://www.astronomie-amateur.fr>

⁴ http://www.astrosurf.com/aras/Aras_DataBase/Symbiotics/AGPeg.htm

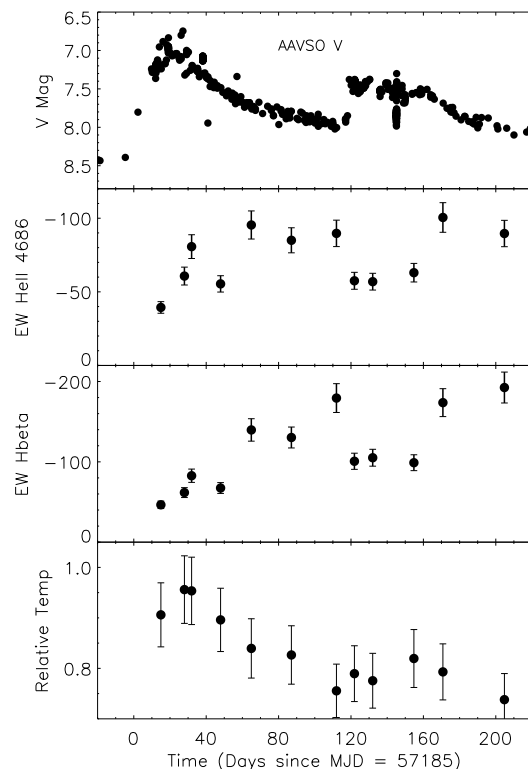


Figure 2. From the top we show the AAVSO V band light curve; the equivalent width of the He II (4686) and H β line (derived using data taken by French amateur astronomers) and the relative effective temperature derived using these lines. As there is some uncertainty over the absolute temperature calibration using this method, we determine the relative temperature over the course of the outburst, where a value of unity implies an effective temperature of 1.9×10^5 K using the formula of Iijima (1981).

Because *Swift* is in a low Earth orbit, each observation sequence (which makes up an ‘ObservationID’) can be made up of more than one pointing, while the total exposure time of the X-ray observation in each ObservationID was typically 1–2 ksec (see Table A1). The XRT (Burrows et al. 2005) on-board *Swift* has a field of view of 23.6×23.6 arcmin with CCD detectors allowing spectral information of X-ray sources to be determined. It is sensitive over the range 0.3–10 keV and at launch had a spectral resolution of 140 eV at 6 keV (which has since degraded over time).

The XRT has a number of modes of operation (designed to observe gamma-ray bursts at various stages of their evolution), but here we concentrate on the ‘photon counting’ mode which has full imaging and spectroscopic information. The data are processed using the standard XRT pipeline and it is these higher level products which we use in our analysis⁵.

3.2 X-ray light curve

To determine the count rate of AG Peg at each epoch we

⁵ http://swift.gsfc.nasa.gov/docs/swift/analysis/xrt_sguide_v1_2.pdf

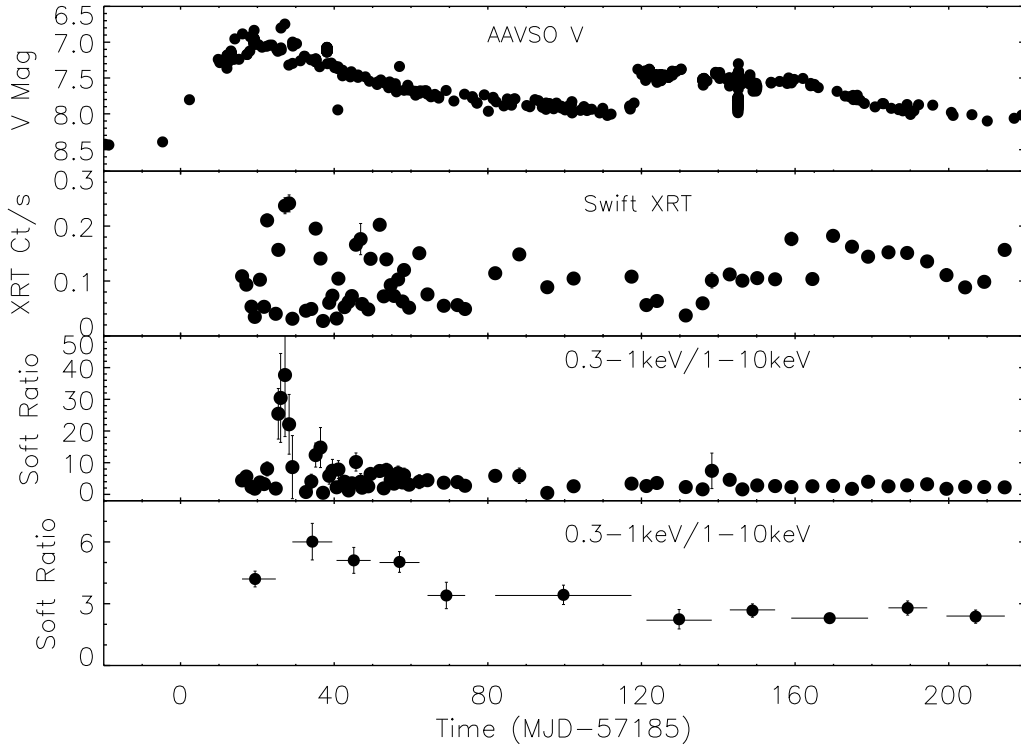


Figure 3. From the top we show: The V magnitude of AG Peg as obtained by AAVSO observers; the X-ray light curve of AG Peg (0.3–10 keV) as derived using *Swift* XRT data; the X-ray softness ratio; and the softness ratio where we have combined a number of epochs of data and (for clarity) we have omitted the epoch with the softest data points.

filtered the X-ray events to extract photons with corresponding ‘grades’ 0–12 (this has the effect of filtering out events which are not from the target) and energy ranges from each ObservationID and made an image using `xselect`⁶. We used the HEASoft tool `XIMAGE` and the routine `SOSTA` (which takes into account effects such as vignetting, exposure and the point spread function) to determine the count rate and error at the position AG Peg. We determined an energy independent correction for each pointing to account for the fact that X-ray photons from AG Peg may have been deposited on known bad columns on the XRT detectors using the tool `xrtlccorr`⁷. We show the count rate as a function of time since the start of the outburst in Figure 3. (The characteristics of the X-ray light curve are very similar whether we apply the correction or not).

The first four epochs of the X-ray observations were made as AG Peg was just approaching maximum optical brightness and show a decreasing X-ray flux (~ 0.07 to 0.01 ct/s). This compares with a count rate of 0.02 – 0.03 ct/s when AG Peg was observed in 2013 Aug using the XRT. The X-ray flux then experiences some epochs of significantly enhanced X-ray rates reaching ~ 0.3 ct/s at MJD=57211 (26 d after the start of the outburst). As AG Peg slowly declines in optical flux the X-ray flux continues to show significant variations, although there is a decline in the peak count rate over this time interval.

As indicated earlier, approximately 120 days after the start of the optical outburst there is an optical rebrightening event where the system increases in brightness by ~ 0.5 mag. In X-rays there is a decline in flux as the system brightens in the optical. However, by the time the system reaches maximum optical brightness and starts to decline, the X-ray flux starts to increase in flux, giving tentative evidence for a delay of ~ 20 days between the X-ray and optical flux, or a suppression of X-rays during the rebrightening episode (Figure 3).

To search for changes in the broad X-ray spectral distribution over the outburst we derived light curves (using the same method as before) for two energy bands: 0.3–1.0 keV and 1–10 keV (for reference we give the count rate in different energy bands in Table A1). We show how the softness ratio (0.3–1.0 keV/1–10 keV) changes over the outburst in Figure 3. It is clear that during the time of highest flux (MJD \sim 57210) the softness ratio is high (i.e. the spectrum is dominated by soft X-ray photons). As the source declines in optical flux, the large day-to-day X-ray flux variations are not reflected in changes to the softness ratio whose changes are much less marked. We also co-added data from different epochs to search for a variation in the softness ratio as the outburst progressed and the results of this are shown in Figure 3. The spectrum of AG Peg appears to harden after the very soft epoch reaching a minimum by the time of the onset of the rebrightening event. During the rebrightening event the softness ratio is roughly constant.

⁶ <http://heasarc.nasa.gov/docs/software/lheasoft/ftools/xselect/xselect.html>

⁷ <http://www.swift.ac.uk/analysis/xrt/lccorr.php>

3.3 X-ray spectra

We now investigate the X-ray spectrum of AG Peg in more detail. Photons were extracted from a circular aperture centered on AG Peg and also a source-free region of the detector to create a background spectrum. We obtain an ancillary file, which allows us to determine the flux of the source, using an exposure map derived from the event files which are used to make up the spectrum. We used the response file, which allows the energy of each photon to be tagged, appropriate to the mode and grade of event, which was taken from the NASA HEASARC site⁸. The source spectrum was binned so that each bin had a minimum of 20 counts.

Using all the data, with the exception of the soft bright state, we obtain a spectrum with a total exposure time of 113.3 ksec. This spectrum is consistent with that of absorbed thermal plasma emission with emission detected up to ~ 3 keV. Mürset et al. (1997) and Luna et al. (2013) classed the X-ray properties of Symbiotic binaries according to the nature and energetics of the spectrum. The integrated spectrum of AG Peg during outburst is similar, for instance, to *Swift* J1719–3002 made during a quiescent state (Luna et al. 2013) which was classed as having a ‘ β ’ spectrum which indicates a spectrum peaking ~ 0.8 keV, with most photons softer than 2.4 keV and is likely produced by a collision of winds from the white dwarf and red giant ($\sim 1/3$ of sources in the study of Luna et al. show a β type spectrum).

Using the X-ray fitting package XSPEC (Dorman & Arnaud 2001), we modelled the integrated spectrum using a range of emission models in combination with the `tbabs` absorption model (Wilms et al. 2000). We found that although a two temperature thermal plasma model gave significantly better fits than a one temperature model it was not formally a good fit ($\chi^2_\nu=2.60$). We allowed various elements to have non-Solar abundances and whilst we obtained formally better fits, it was not a formally acceptable fit ($\chi^2_\nu=1.59$). In addition, there was some concern that we were obtaining non-physical abundances and therefore fitting noise in the spectrum.

The observed flux inferred from this model is 1.3×10^{-12} erg s⁻¹ cm⁻² (0.3–10 keV); the unabsorbed flux in the same band is 1.9×10^{-12} erg s⁻¹ cm⁻², giving an X-ray luminosity, assuming a distance of 1 kpc (interferometric observations show AG Peg to have a parallax less than 1 mas, Boffin et al. 2014) of $L_X \sim 2.3 \times 10^{32}$ erg/s (which is typical for symbiotic stars in a quiescent state, c.f. Luna et al. 2013).

It is clear from the softness ratio shown in Figure 3 that the X-ray spectrum is much softer ~ 25 days after the start of the outburst. We extracted a spectrum from this soft phase and for comparison, we extracted a spectrum from data taken from pointings made in the next 30 days after this (the ‘high’ phase). We show the X-ray spectrum taken from the soft and high phases in Figure 4. There is no evidence for a soft blackbody component in the ‘soft’ spectrum – rather the soft spectrum was best fit by a single thermal plasma model whilst the high spectrum was best fit using two thermal plasma models. The difference between the ‘soft’ and ‘high’ spectra was not due to different amounts of absorption. However, the goodness of fits to both spectra

were still not formally acceptable ($\chi^2_\nu=2.28$ and $\chi^2_\nu=1.63$ for the soft and high spectra respectively). We therefore do not provide additional details of the fits.

4 DISCUSSION

The 2015 outburst of AG Peg is the first to be observed since the mid 19th century. The duration and amplitude of these outbursts are very different in the optical, with the most recent being much shorter and of lower amplitude compared to the earlier outburst. We now discuss the physical reasons for these differences, the origin of the X-ray emission, and the generation of quasi-steady nuclear burning on the white dwarfs in AG Peg and other symbiotic binaries.

4.1 The nature of the 2015 outburst

The ‘slow-nova’ outburst of AG Peg in the mid 19th century was almost certainly driven by a TNR on the surface of the accreting white dwarf (e.g. Gallagher et al. 1979, Kenyon et al. 1993). In contrast, the double-peaked 2015 outburst was much less energetic and of shorter duration. Moreover, whereas optical spectra taken during the decline of the slow-nova showed only absorption lines due to the expanded white dwarf photosphere (Gallagher et al. 1979), optical spectra during the 2015 eruption⁹ displayed emission lines such as O VI (indicating highly ionized species in the nebula) which imply that material was still being exposed to the photoionizing hot white dwarf.

Rather than mimicking a slow-nova, the 2015 outburst appeared more similar to *classical* symbiotic outbursts which have time scales of months to years (for instance Z And or AG Dra). The coverage of the optical photometry during the rise to optical maximum was not high enough to reveal whether the eruption was triggered by an accretion-disk instability, as in Z And. However, the optical light curve of Z And during the 2000–2002 event (shown in Sokoloski et al. 2006), also shows a rebrightening event and is remarkably like AG Peg, the difference being that in Z And the outburst lasted 2 years rather than 6 months in the case of AG Peg. The re-brightening event is also reminiscent of brightness oscillations seen in classical symbiotic outbursts in e.g. CI Cyg, AX Per, and AG Dra (Mikolajewska & Kenyon 1992; Viotti et al. 2005), which some authors have speculated could be driven by resonances in an accretion disk. The modest increase in X-ray flux averaged over the 2015 event is also consistent with the increases in X-ray flux from Z And during its classical symbiotic outburst.

4.2 The origin of the X-ray emission

It is thought that classical outbursts from symbiotics may be driven by a disk instability, of the sort which drives dwarf nova outbursts, which can increase the rate of quasi-steady nuclear shell burning on the white dwarf (Sokoloski et al. 2006). However, whereas almost all dwarf nova outbursts in CVs show a suppression of X-rays as the boundary layer

⁸ http://swift.gsfc.nasa.gov/proposals/swift_responses.html

⁹ e.g. http://www.astrosurf.com/aras/novae/InformationLetter/ARAS_EruptiveStars_2016-01.pdf

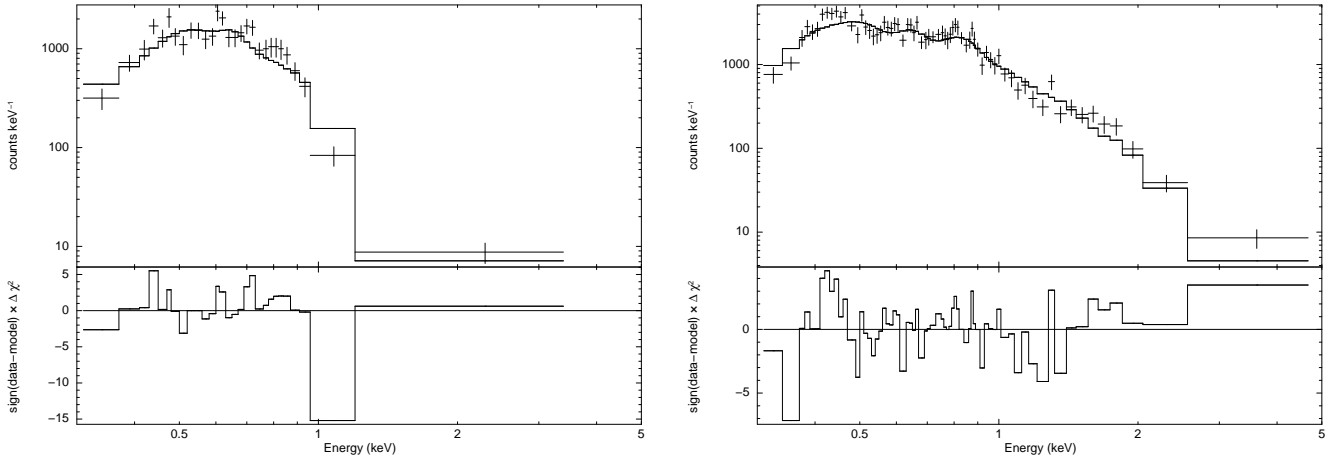


Figure 4. On the left hand side we show the X-ray spectrum taken during the soft X-ray phase and on the right the X-ray spectrum taken immediately after this (the ‘high’ phase). The model best fit is shown as a solid line and is an two temperature absorbed thermal plasma model.

between the accretion disk and the white dwarf becomes optically thick (with temperatures of just a few tens of eV; Wheatley et al. 1996), the connection between X-ray emission and the underlying physics is less clear in most classical symbiotic outbursts. In symbiotic stars with quasi-steady shell burning on the white dwarf, the accretion disk does not produce detectable X-ray emission because UV photons from the hot white dwarf Compton cool the boundary layer out of the X-ray regime (e.g., Luna et al. 2013). As discussed in §4.3, there is evidence that the white dwarf in AG Peg hosted shell burning throughout the 2015 eruption.

The temperature of the X-ray emission in AG Peg is much lower than the temperatures typically seen in dwarf novae in quiescence (~ 10 keV) – consistent with the idea that the X-ray emitting plasma in AG Peg was not located near the surface of the white dwarf, deep within its potential well. Our spectral models indicate temperatures below 1 keV. Super-Soft X-ray emission is commonly seen after outbursts from novae and occasionally from symbiotics (e.g. AG Dra, Skopal et al. 2009). However, as expected for a low-mass white dwarf with quasi-steady shell burning, no super-soft X-ray emission was detected in AG Peg, confirming that nuclear burning did not lead to a white dwarf photosphere which was hot enough for blackbody emission to be seen in the supersoft X-rays.

One of the characteristics of the X-ray observations of AG Peg is the high day-to-day variability. X-ray observations of AG Peg started with *Swift* shortly before it reached peak optical brightness. They show that around 20–30 days after the optical peak, the X-ray emission became strongly variable on a timescale shorter than a day and that the spectrum became soft for a handful of days. As AG Peg continued to fade in the optical, the X-ray flux continued to show day to day variations but the spectrum started to harden. At the time of the optical re-brightening event the X-ray flux reduced to very low levels until it started to increase after around 10 days. The degree of variability reduced and the hardness of the spectrum remained roughly constant.

Given that the level of absorption did not show an overall decrease over the course of the outburst – as one might ex-

pect for the clearing of ejecta – we do not find evidence that the day-to-day variability was due to changing levels of absorption from a clumpy outflow. However, we do expect that shocks were generated in the AG Peg outburst as ejecta interacted with circumbinary material (see e.g. Mürset, Wolff & Jordan 1977, Pan, Ricker & Taam 2015). In an extreme case of such interactions, the 2006 outburst of RS Oph triggered a shock wave that was seen at multiple wavelengths (e.g., O’Brien et al. 2006). In the 2000–2002 outburst of Z And, a jet was seen at radio wavelengths (Brocksopp et al. 2004), and it is known that jets from symbiotic binaries can produce faint X-rays (e.g., Galloway & Sokolowski 2004; Karovska et al. 2007, 2010, Kellogg et al. 2007, Nichols et al. 2007). Evidence for winds in symbiotic binaries, including AG Peg (Nussbaumer et al. 1995), is widespread. The optical spectra discussed in §2.2 show evidence for extended wing features in the Balmer line emission during the 2015 outburst. For X-ray temperatures < 1 keV, we would expect shock speeds slower than 1000 km/s (see eqn 4 of Stute, Luna & Sokolowski 2011), consistent with the optical line widths. Taking a Bremsstrahlung cooling time of:

$$t_{\text{Brems}} = \left(\frac{T}{2} \times 10^6 \text{K}\right)^{1/2} \left(\frac{n}{3} \times 10^9 \text{cm}^{-3}\right) \sim \text{days} \quad (1)$$

(Frank, King, & Raine 1992), the rapid X-ray variability suggests that the shocked gas was probably quite dense. Alternatively, if the rapid variability was due to adiabatic-expansion cooling of shocked clumps, the clumps must have been less than $\sim 10^{12}$ cm (or $\sim 1/10$ of an AU) in size. High densities and small clump sizes are both plausible, so the rapid X-ray variability is consistent with our hypothesis that the X-ray emission was due to shocks associated with a (perhaps collimated) eruptive outflow.

Approximately 120 days after the start of the outburst, the optical flux brightened by $V \sim 0.5$ mag in less than a day, after which it showed a gradual decline over ~ 40 days followed by a more rapid decline. A rebrightening event was also seen in the 2000–2002 outburst of Z And which was attributed to a decrease in the temperature of the optical emitting material due to a slight expansion of the white dwarf

photosphere (Sokoloski et al. 2006). However, the temperature derived from the He II and H β lines (Figure 2) suggest the temperature did not change significantly over the course of the rebrightening event. The *Swift* observations of AG Peg show a suggestion of a ~ 20 day delay between the initial rise of the optical and X-ray fluxes at this epoch.

Compared to dwarf nova outbursts, symbiotic binaries show a greater diversity of X-ray/optical characteristics over an outburst cycle. AG Dra, whose 1994–1995 outburst was driven by an expansion of the photosphere of the shell-burning white dwarf, showed a clear drop in X-ray flux (0.1–2.4 keV) during an optical outburst (Greiner et al. 1997). On the other hand the symbiotic star V407 Cyg shows an *increase* in the 0.3–10 keV flux around 20 days after an outburst in 2010 in which ejecta collided with circumbinary material (Nelson et al. 2012). Based on the similarity between the optical light curves of AG Peg and Z And, we suggest that the 2015 outburst of AG Peg was also triggered by an accretion instability. Based on the properties of the X-ray emission, we suggest that enough material was ejected during the outburst to heat ejecta and/or circumbinary material through shocks.

4.3 Origin of quasi-steady shell burning in classical symbiotic stars

Mürset et al. (1991) and Skopal (2005) modelled UV spectra of a sample of symbiotic stars obtained using *IUE* and found white dwarf temperatures and luminosities around $\sim 10^5$ K and $\sim 10^3 L_{\odot}$ respectively — much higher than expected from accretion alone. Because nuclear burning releases 40 to 50 times more energy per nucleon than accretion onto a white dwarf, these high temperatures and luminosities are naturally explained if shell burning is present. Given that shell burning is not a common (long-term) feature of accreting white dwarfs in CVs, why is it so frequently present in symbiotic stars?

Two main possibilities exist for the origin of quasi-steady shell burning in normal white dwarf symbiotics. It could be the result of accretion at a rate above the theoretical minimum for shell burning but below the value that leads to expansion of the white dwarf envelope to giant dimensions (Paczynski & Żytkow 1978; Sion, Acierno, & Tomczyk 1979; Paczynski & Rudak 1980; Fujimoto 1982a; Nomoto 1982a,b, Iben 1982). One problem with this scenario, however, is that the range of accretion rates that produce steady burning is narrow (a factor of a few, Fujimoto 1982b), and it seems unlikely that most symbiotic stars accrete at a rate just within this range. The other alternative is that the observed quasi-steady shell burning is residual burning from a prior nova.

The lower limits that Swift/UVOT placed on the UV flux during the 2015 event attest to the continued presence of shell burning on the surface of the white dwarf while it experienced classical symbiotic eruptions. The *Swift*/UVOT saturates through the UVW2 filter at around 12.6 mag (in the AB system¹⁰), which corresponds to a flux density at 1928 Å of 2.75×10^{-13} erg s $^{-1}$ cm $^{-2}$ Å $^{-1}$. Multiplying this value by the UVW2 filter width of 657 Å (Poole et al. 2008),

dereddening it using the $E(B - V) = 0.1$ (Kenyon et al. 1993), and taking a distance of at least 1 kpc (Boffin et al. 2014), we find a luminosity between approximately 1600Å and 2260Å of at least 4.3×10^{34} erg s $^{-1}$. The presence of the Raman-scattered O VI line (at 6825Å) throughout the 2015 eruption indicates that the temperature of the hot white dwarf remained above 110,000 K (Mürset & Nussbaumer 1994). We therefore multiply the 1600–2260Å luminosity by a factor of 5 as a conservative bolometric correction (for a white dwarf that either hosts shell burning or accretes at a very high rate). Keeping in mind that both the UVOT flux and the distance are lower limits, we conclude that the luminosity of either the white dwarf or the accretion disk was likely well in excess of $\sim 2 \times 10^{35}$ erg s $^{-1}$ during the recent outburst.

For the disk to have produced this luminosity it would have required an accretion rate above $\sim 10^{-7} M_{\odot}$ yr $^{-1}$. It is theoretically challenging, however, for a 0.6 M_{\odot} white dwarf to accrete at such a high rate without generating quasi-steady shell burning (Paczynski & Żytkow 1978; Nomoto 1982a). As in other classical symbiotic stars, such as Z And and AG Dra, the most natural interpretation is that quasi-steady shell burning remains present on the surface of the white dwarf.

AG Peg’s transition from a slow nova to a classical symbiotic, marked by classical symbiotic outbursts, suggests that shell burning in at least some (and perhaps most) symbiotics with strong optical emission lines is residual burning from prior novae outbursts. That the luminosity of the white dwarf in AG Peg was very low before the 19th century slow nova (Mürset & Nussbaumer 1994) confirms that material was not burning on the white dwarf before that event. After the start of the slow nova, however, the temperature and luminosity were consistently high enough to indicate shell burning (Mürset & Nussbaumer 1994). In fact, the slow nova led to a prolonged period of burning that persisted through the recent active phase. The lack of any hard X-ray emission from the accretion-disk boundary layer in 2013 (despite AG Peg’s distance of only about 1 kpc and its extreme UV brightness; Nuñez & Luna 2013) supports the notion that shell burning was present through 2013.

As we argued above, the continued UV brightness throughout the recent period of optical activity implies that shell burning is on-going. Interestingly, RX Pup, which has been identified as a symbiotic slow nova by Mikolajewska et al. (2002), also experienced an optical rebrightening. If the steady burning in other symbiotic stars is also the result of prior novae, it would follow that accretion onto the white dwarf in these systems does not necessarily proceed at the rate required for quasi-steady shell burning. Shell burning arising from prior novae would also have implications for selection biases in the sample of known symbiotic stars and the efficiency with which symbiotic white dwarfs can retain accreted material.

5 SUMMARY AND CONCLUSIONS

The optical outburst of AG Peg in 2015 had a lower amplitude and much shorter duration than the outburst observed in the mid 19th century. The earlier event was very likely driven by a TNR on the surface of the white dwarf. In con-

¹⁰ http://swift.gsfc.nasa.gov/analysis/uvot_digest/coiloss.html

trast, the recent event is similar to classical symbiotic outbursts in which an accretion instability dumps fuel onto an already burning white dwarf. The optical light curve of AG Peg is very similar (if taking place over a shorter timescale) to the 2000–2002 outburst of Z And. The X-ray observations show strong soft X-ray emission which has large day-to-day variations 20–30 days after outburst. The X-ray flux continued to show marked day-to-day variations for another month. This variability is similar to that seen in some novae such as RS Oph which is thought to be due to shocks interacting with clumpy material in the ejecta and emitting X-rays. There is also evidence that the optical rebrightening event showed X-rays being delayed by ~ 20 days compared to the optical, hinting that material had to clear in order for the X-rays to be seen. Irrespective of the exact causes of the 2015 outburst of AG Peg and its X-ray emission, it is clear that AG Peg has stopped behaving like a slow nova and started behaving like a classical symbiotic star. With this transition, AG Peg provides support for the idea that quasi-steady shell burning on the white dwarfs in symbiotic stars is residual burning from prior novae.

6 ACKNOWLEDGMENTS

We warmly thank the *Swift* PI Neil Gehrels and his team for approving our observations and scheduling them. We acknowledge with thanks the variable star observations from the AAVSO International Database contributed by observers worldwide and used in this research. We also thank François Teyssier for altering us to the many amateur spectroscopic observations which have been made and we acknowledge and thank François Teyssier, Umberto Sollecchia, Joan Guarro Flo, Jacques Montier, Peter Somogyi, Keith Graham and V Bouttard for use of their spectra. Armagh Observatory is supported by the Northern Ireland Government through the Dept of Culture, Arts and Leisure. GJML and NEN acknowledge support from Argentina grant ANPCYT-PICT 0478/14. GJML and NEN are members of the "Carrera del Investigador Científico (CIC)" of CONICET. We thank the referee for a helpful and constructive report.

REFERENCES

- Allen, D. A., 1980, MNRAS, 192, 521
 Allen, D. A., 1981, MNRAS, 197, 739
 Allen, D. A., 1984, Ap&SS, 99, 101
 Belczyński, K., Mikołajewska, J., Munari, U., Ivison, R. J., Friedjung, M., 2000, A&AS, 146, 407
 Belyakina, T. S., 1968, SvA, 110
 Boffin, H. M. J., Hillen, M., Berger, J. P., Jorissen, A., Blind, N., Le Bouquin, J. B., Mikołajewska, J., Lazareff, B., 2014, A&A, 564, 1
 Brocksopp, C., Sokoloski, J. L., Kaiser, C., Richards, A. M., Muxlow, T. W. B., Seymour, N. 2004, MNRAS, 347, 430
 Burrows, D. N., et al, 2005, SSRv, 120, 165
 Corradi, R. L. M., et al., 2008, A&A, 480, 409
 Corradi, R. L. M., et al., 2010, A&A, 509, 41
 Dilday, B., et al., 2012, Sci, 337, 942
 Di Stefano, R., 2010, ApJ, 719, 474
 Dorman, B., Arnaud, K. A., 2001, in *Astronomical Data Analysis Software and Systems X*, ASP Conference Proceedings, Vol. 238. Ed F. R. Harnden, Jr., Francis A. Primini, Harry E. Payne., San Francisco: ASP, p.415
 Fekel, F. C., Joyce, R. R., Hinkle, K. H., Skrutskie, M. F., 2000, AJ, 19, 1375
 Frank, J., King, A., & Raine, D. J. 2002, *Accretion Power in Astrophysics*, Cambridge University Press, 2002.
 Fujimoto, M. Y., 1982a, ApJ, 257, 752
 Fujimoto, M. Y., 1982b, ApJ, 257, 767
 Gallagher, J. S., Webbink, R. F., Holm, A. V., Anderson, C. M., 1979, ApJ, 229, 994
 Galloway, D. K., Sokoloski, J. L., 2004, ApJ, 613, L61
 Gehrels, N., et al. 2004, ApJ, 611, 1005
 Greiner, J., Bickert, K., Luthardt, R., Viotti, R., Altamore, A., Gonzalez-Riestra, R., Stencel, R. E., 1997, A&A, 322, 576
 Iben, I., 1982, ApJ, 259, 244
 Iben, I., Tutukov, A. V., 1996, ApJS, 105, 145
 Iijima, T. 1981, in *Photometric and Spectroscopic Binary Systems*, ed. E. B. Carling & Z. Kopal, Dordrecht, Kluwer, 517
 Kafka, S., 2015, Observations from the AAVSO International Database, <http://www.aavso.org>
 Karovska, M., Carilli, C. L., Raymond, J. C., Mattei, J. A., 2007, ApJ, 661, 1048
 Karovska, M., Gaetz, T. J., Carilli, C. L., Hack, W., Raymond, J. C., Lee, N. P., ApJ, 2010, 710, L132
 Kellogg, E., Anderson, C., Korreck, K., DePasquale, J., Nichols, J., Sokoloski, J. L., Krauss, M., Pedelty, J., 2007, ApJ, 664, 1079
 Kenyon, S. J., Truran, J. W., 1983, ApJ, 273, 280
 Kenyon, S. J., Webbink, R. F., 1984, ApJ, 279, 252
 Kenyon, S. J. Fernandez-Castro, T., 1987, AJ, 93, 938
 Kenyon, S. J., Mikołajewska, J., Mikołajewski, M., Polidan, R. S., Slovak, M. H., 1993, AJ, 106, 1573
 Kenyon, S. J., Proga, D., Keyes, C. D., 2001, AJ, 122, 349
 Luna, G. J. M., Sokoloski, L. J., Mukai, K., Nelson, T., 2013, A&A, 559, 6
 Luna, G. J. M., Nuñez, E. N., Sokoloski, L. J., Montane, B., 2015, ATel, 7741
 Merrill, P. W., 1951, ApJ, 113, 605
 Mikołajewska, J., 2007, Baltic Astron., 16, 1
 Mikołajewska, J., Kenyon, S., 1992, MNRAS, 256, 177
 Mikołajewska, J., Brandi, E., Garcia, L., Ferrer, O., Quiroga, C., Anupama, G. C., 2002, In *Classical Novae Explosions*, Eds M. Hernanz, J. Jose, AIP Conf Proc., 637, 42
 Munari, U., Valisa, P., Dallaporta, S., Cherini, G., Righetti, G. L., Castellani, F., 2013 ATel 5258
 Mürset, U., Nussbaumer, H., Schmid, H. M., Vogel, M., 1991, A&A, 248, 458
 Mürset, U., Nussbaumer, H., 1994, A&A, 282, 586
 Mürset, U., Wolff, B., Jordan, S., 1997, A&A, 319, 201
 Nelson, T., Donato, D., Mukai, K., Sokoloski, J., Chomiuk, L., 2012, ApJ, 74, 43
 Nichols, J. S., DePasquale, J., Kellogg, E., Anderson, C. S., Sokoloski, J., Pedelty, J., 2007, ApJ, 660, 651
 Nomoto, K., 1982a, ApJ, 253, 798
 Nomoto, K., 1982b, ApJ, 257, 780
 Nuñez, N. E., & Luna, G. J. M., 2013, ATel 5324
 Nussbaumer, H., Schmutz, W., Vogel, M., 1995, A&A, 293, L13
 O'Brien, T., et al., 2006, Nature, 442, 279
 Pan, K.-C., Ricker, P. M., Taam, R. E., 2015, ApJ, 806, 27
 Paczynski, B., Zytkow, A. N., 1978, ApJ, 222, 604
 Paczynski, B., Rudak, B., 1980, A&A, 82, 349
 Poole, T. S., et al., 2008, MNRAS, 383, 627
 Ramsay, G., Wheatley, P. J., Rosen, S., Barclay, T., Steeghs, D., 2012, MNRAS, 425, 1486
 Ramsay, G., Luna, G. J. M., Nuñez, E. N., Sokoloski, L. J., Montane, B., 2015, ATel, 7779
 Rigollet, R., 1947, L'Astronomie, 61, 54

- Rodríguez-Flores, E. R., et al., 2014, *A&A*, 567, 49
Skopal, A., 2005, *A&A*, 440, 995
Skopal, A., Sekeráš, M., González-Riestra, R., Viotti, R. F., 2009, *A&A*, 507, 1531
Sion, E. M., Acierno, M. J., Tomczyk, S., 1979, *ApJ*, 230, 832
Sokoloski, J. L., et al., 2006, *ApJ*, 636, 1002
Steele, I. A., Jermak, H. E., Marchant, J. M., Bates, S. D., 2015, *ATel*, 7749
Stute, M., Luna, G. J. M., Sokoloski, J. L., 2011, *ApJ*, 731, 12
Viotti, R., et al., 2005, *Ap&SS*, 296, 435
Waagen, E.O., 2015, *AAVSO Alert Notice*, 521
Wheatley, P. J., Verbunt, F., Belloni, T., Watson, M. G., Naylor, T., Ishida, M., Duck, S. R., Pfeffermann, E., 1996, *A&A*, 307, 137
Wilms, J., Allen, A., McCray, R., 2000, *ApJ*, 542, 914

APPENDIX A: TABLES

Table A1. The observation log for the *Swift* XRT observations. We indicate the Observation ID (ObsID); the start of the observations; the time since the optical outburst (defined as MJD=57185 = 2015 June 12); the duration of the XRT exposure and then the observed count rate and error (1σ) in the 0.3–10 keV, 0.3–1 keV and 1–10 keV energy bands. We have applied a correction to take into account that some fraction of the source PSF make have overlapped with dead columns on the detector (see text for details).

ObsID	Start Time (MJD)	Time from Outburst (d)	XRT Exp (s)	0.3-10 keV (Ct/s)	\pm	0.3-1 keV (Ct/s)	\pm	1–10 keV (Ct/s)	\pm
00032906003	57201.017	16.0	8949	0.1140	0.0045	0.0868	0.0040	0.0197	0.0019
00032906004	57202.128	17.1	1923	0.0951	0.0078	0.0809	0.0072	0.0143	0.0030
00032906005	57203.466	18.5	1627	0.0457	0.0006	0.0321	0.0050	0.0136	0.0033
00032906006	57204.324	19.3	1555	0.0227	0.0044	0.0143	0.0034	0.0080	0.0025
00032906007	57205.667	20.7	1916	0.1063	0.0086	0.0791	0.0074	0.0209	0.0038
00032906008	57206.735	21.7	2018	0.0454	0.0047	0.0392	0.0044	0.0121	0.0025
00032906009	57207.535	22.5	1419	0.2395	0.0140	0.2144	0.0140	0.0267	0.0048
00032906011	57209.784	24.8	1978	0.0297	0.0036	0.0203	0.0030	0.0111	0.0022
00032906012	57210.450	25.4	4864	0.1732	0.0062	0.1620	0.0060	0.0064	0.0012
00032906013	57211.055	26.1	903	0.3954	0.0250	0.3803	0.0240	0.0125	0.0044
00032906014	57212.191	27.2	1221	0.2724	0.0180	0.2602	0.0180	0.0069	0.0029
00032906015	57213.258	28.3	1091	0.2776	0.0190	0.2618	0.0190	0.0118	0.0040
00032906016	57214.117	29.1	1622	0.0186	0.0033	0.0168	0.0031	0.0020	0.0011
00032906018	57217.645	32.6	1273	0.0366	0.0062	0.0165	0.0042	0.0221	0.0048
00032906019	57219.042	34.0	1088	0.0406	0.0072	0.0325	0.0064	0.0080	0.0032
00032906020	57220.170	35.2	1715	0.2210	0.0130	0.1995	0.0130	0.0161	0.0036
00032906021	57221.429	36.4	1815	0.1538	0.0096	0.1411	0.0091	0.0095	0.0024
00032906022	57222.095	37.1	2399	0.0136	0.0023	0.0068	0.0017	0.0136	0.0024
00032906023	57223.699	38.7	1602	0.0544	0.0069	0.0476	0.0065	0.0081	0.0027
00032906024	57224.543	39.5	1294	0.0704	0.0089	0.0607	0.0082	0.0081	0.0030
00032906025	57225.627	40.6	1971	0.0191	0.0040	0.0151	0.0035	0.0068	0.0024
00032906026	57226.093	41.1	1822	0.1087	0.0100	0.0935	0.0094	0.0119	0.0033
00032906027	57227.684	42.7	1896	0.0447	0.0055	0.0356	0.0049	0.0089	0.0024
00032906028	57228.748	43.7	1013	0.0564	0.0079	0.0312	0.0058	0.0252	0.0053
00032906029	57229.598	44.6	1976	0.0695	0.0067	0.0434	0.0053	0.0124	0.0028
00032906030	57230.668	45.7	1863	0.1848	0.0120	0.1555	0.0110	0.0152	0.0035
00032906032	57231.883	46.9	2006	0.1975	0.0350	0.1477	0.0310	0.0368	0.0150
00032906033	57232.271	47.3	1361	0.0517	0.0073	0.0340	0.0059	0.0161	0.0041
00032906034	57233.868	48.9	1690	0.0397	0.0062	0.0319	0.0055	0.0125	0.0035
00032906035	57234.468	49.5	1193	0.1532	0.0130	0.1294	0.0120	0.0201	0.0048
00032906036	57236.847	51.8	1951	0.2296	0.0110	0.2037	0.0100	0.0276	0.0037
00032906037	57237.911	52.9	1943	0.0689	0.0068	0.0443	0.0055	0.0233	0.0040
00032906039	57238.588	53.6	1931	0.1519	0.0110	0.1232	0.0098	0.0160	0.0035
00032906041	57239.712	54.7	2016	0.0940	0.0071	0.0704	0.0061	0.0154	0.0029
00032906042	57240.572	55.6	1963	0.0698	0.0071	0.0698	0.0071	0.0207	0.0039
00032906043	57241.636	56.6	1931	0.1068	0.0089	0.0746	0.0074	0.0112	0.0029
00032906044	57242.780	57.8	1968	0.0574	0.0070	0.0455	0.0062	0.0121	0.0032
00032906045	57243.179	58.2	1755	0.1280	0.0110	0.0794	0.0088	0.0131	0.0036
00032906046	57244.498	59.5	2064	0.0435	0.0049	0.0287	0.0039	0.0094	0.0023
00032906047	57247.154	62.2	313	0.1657	0.0029	0.1400	0.0270	0.0350	0.0130
00032906048	57249.283	64.3	1900	0.0733	0.0072	0.0590	0.0065	0.0132	0.0031
00032906050	57253.539	68.5	2094	0.0477	0.0055	0.0379	0.0049	0.0103	0.0025
00032906052	57257.089	72.1	1843	0.0492	0.0063	0.0370	0.0054	0.0095	0.0027
00032906053	57259.060	74.1	1707	0.0405	0.0060	0.0333	0.0054	0.0122	0.0033
00032906054	57266.924	81.9	1454	0.1208	0.0110	0.1019	0.0100	0.0174	0.0042
00032906055	57273.188	88.2	935	0.1631	0.0130	0.1275	0.0011	0.0217	0.0046
00032906056	57280.477	95.5	2028	0.0894	0.0067	0.0148	0.0027	0.0320	0.0040
00032906057	57287.333	102.3	2006	0.1089	0.0098	0.0768	0.0082	0.0299	0.0051
00032906058	57302.421	117.4	948	0.1131	0.0130	0.0890	0.0120	0.0263	0.0064
00032906059	57306.285	121.3	970	0.0493	0.0092	0.0576	0.0099	0.0218	0.0061
00032906060	57309.006	124.0	1835	0.0585	0.0066	0.0446	0.0057	0.0124	0.0030
00032906061	57316.531	131.5	707	0.0259	0.0074	0.0207	0.0066	0.0090	0.0043
00032906062	57320.926	135.9	1424	0.0533	0.0073	0.0290	0.0054	0.0182	0.0043
00032906063	57323.331	138.3	496	0.1048	0.0170	0.0713	0.0140	0.0096	0.0050
00032906064	57327.971	143.0	1492	0.1181	0.0110	0.0957	0.0098	0.0208	0.0045

Table A1. Cont ...

ObsID	Start Time (MJD)	Time from Outburst (d)	XRT Exp (s)	0.3-10 keV (Ct/s)	±	0.3-1 keV (Ct/s)	±	1-10 keV (Ct/s)	±
00032906065	57331.282	146.3	1387	0.1041	0.0100	0.0620	0.0081	0.0391	0.0064
00032906066	57335.138	150.1	2287	0.1098	0.0081	0.0818	0.0069	0.0289	0.0041
00032906067	57339.794	154.8	2141	0.1072	0.0094	0.0684	0.0069	0.0260	0.0042
00032906068	57344.048	159.0	1094	0.1977	0.0150	0.1380	0.0120	0.0598	0.0081
00032906069	57349.504	164.5	2000	0.1078	0.0089	0.0747	0.0074	0.0291	0.0046
00032906070	57354.884	169.9	1950	0.2048	0.0130	0.1338	0.0100	0.0501	0.0062
00032906071	57359.806	174.9	1783	0.1803	0.0100	0.1082	0.0078	0.0619	0.0059
00032906072	57364.003	179.1	1893	0.1579	0.0110	0.1262	0.0098	0.0317	0.0049
00032906073	57369.315	184.4	1865	0.1678	0.0120	0.1118	0.0100	0.0436	0.0063
00032906074	57374.169	189.4	1900	0.1663	0.0110	0.1206	0.0094	0.0424	0.0056
00032906075	57379.371	194.6	1908	0.1474	0.0110	0.1114	0.0092	0.0348	0.0052
00032906076	57384.412	199.6	1034	0.1166	0.0140	0.0711	0.0110	0.0405	0.0081
00032906077	57389.268	204.5	1401	0.0890	0.0088	0.0716	0.0075	0.0302	0.0052
00032906078	57394.244	209.5	1968	0.1014	0.0093	0.0766	0.0081	0.0329	0.0053
00032906079	57399.563	214.8	1778	0.1732	0.0110	0.1193	0.0089	0.0537	0.0060